HAL
open science

# Comparison of patient-ventilator interfaces based on their computerized effective dead space.

Redouane Fodil, François Lellouche, Jordi Mancebo, Gabriela Sbirlea-Apiou, Daniel Isabey, Laurent Brochard, Bruno Louis

## To cite this version:

Redouane Fodil, François Lellouche, Jordi Mancebo, Gabriela Sbirlea-Apiou, Daniel Isabey, et al.. Comparison of patient-ventilator interfaces based on their computerized effective dead space.: Interface dead space in non-invasive ventilation. Intensive Care Med, 2011, 37 (2), pp.257-62. 10.1007/s00134-010-2066-3 . inserm-00595406

**HAL Id: inserm-00595406**

**https://inserm.hal.science/inserm-00595406**

Submitted on 24 Nov 2011

**HAL** is a multi-disciplinary open access archive for the deposit and dissemination of scientific research documents, whether they are published or not. The documents may come from teaching and research institutions in France or abroad, or from public or private research centers.

L'archive ouverte pluridisciplinaire **HAL**, est destinée au dépôt et à la diffusion de documents scientifiques de niveau recherche, publiés ou non, émanant des établissements d'enseignement et de recherche français ou étrangers, des laboratoires publics ou privés.

Author manuscript, published in "Intensive Care Med 2011;37(2):257-62"
DOI : 10.1007/s00134-010-2066-3



# COMPARISON OF PATIENT-VENTILATOR INTERFACES BASED ON THEIR COMPUTERIZED EFFECTIVE DEAD SPACE

R. Fodil[1,2], F. Lellouche[3], J Mancebo[4], G Sbirlea-Apiou[1,2], D Isabey[1,2], L. Brochard[1,2,5], B. Louis[1,2]

(1) Inserm Unite U955, Cell and Respiratory Biomechanics Group, Créteil, F-94010, France ;
(2) Université Paris-Est, Faculté de Médecine, UMR_S955, Créteil, F-94010, France ;
(3) Université Laval, Centre de Recherche de l'Institut Universitaire de Cardiologie et de Pneumologie de Québec, G1V4G5 Québec, QC, Canada ;
(4) Servei Medicina Intensiva, Hospital Sant Pau, Barcelona, Spain
(5) AP-HP, Groupe Henri-Mondor Albert-Chenevier, Service de Réanimation Médicale, Créteil, F-94010 France ;

Running head : Interface dead space in non-invasive ventilation

Corresponding Author:
Bruno Louis
Inserm U955, Eq. 13
Faculté de Médecine
8 rue du général Sarrail
94010 Créteil Cedex
France

Tel: 33 1 49 81 36 76
Fax: 33 1 48 98 17 77
e-mail: bruno.louis@inserm.fr

Key words: interfaces/masks; non-invasive ventilation; dead space

inserm-00595406, version 1 - 24 May 2011

inserm-00595406, version 1 - 24 May 2011

**ABSTRACT (249 words)**

*Purpose:* Non-invasive ventilation is largely used to treat acute and chronic respiratory failure. This ventilation encounters a non negligible rate of failure related to the used interface/mask, but the reasons for this failure remain unclear. In order to shed light into this issue and to better understand the effects of the geometrical design of interfaces, we aimed to quantify flow, pressure and gas composition in terms of $CO_2$ and $O_2$ at the passage through different types of interface (oronasal mask, integral mask and helmet). Especially, we postulated that due to specific gas flow passing throughout interface, the effective dead space added by the interface is not always related to the whole gas volume included in the interface.

*Methods:* Numerical simulations, using computational fluid dynamics, were used to describe pressure, flow and gas composition during ventilation with the different interfaces.

*Results:* Between the different interfaces the effective dead spaces differed only modestly (110 to 370ml) while their internal volumes were markedly different (110 to 10000ml). It was limited to half the tidal volume for the most voluminous interface, while it was close to the interface gas volume for the less voluminous interfaces. Pressure variations induced by the flow ventilation throughout the interface were negligible.

*Conclusions:* Effective dead space is not related to the internal gas volume included in the interface, suggesting that this internal volume should not be considered as a limiting factor for their efficacy during non-invasive ventilation. Patient's comfort and synchrony have also to be taken into account.

inserm-00595406, version 1 - 24 May 2011

## INTRODUCTION

Non-invasive ventilation (NIV) defines a method of mechanical ventilation that does not require endotracheal intubation. Using this technique, pressurized gas is delivered to the airways through one of a variety of interfaces, such as a mouthpiece or a nasal or facial mask. Over the last two decades, the use of NIV has increased markedly in the treatment of both acute and chronic respiratory failure [1, 2]. In an acute setting, NIV reduces the risk of endotracheal intubation [3] and facilitates the weaning process from mechanical ventilation [4]. Nevertheless for various reasons, NIV is not always successful. The rate of failure for this procedure in acute patients ranges from 7% to 49% [2, 5-7]. One of the reasons reported in the literature to explain this failure rate is the poor patient tolerance to the NIV interface [8, 9]. Mask discomfort, sensation of excessive air pressure, intolerance, skin lesions, leakage and rebreathing have been cited as the most relevant parameters to explain the interface-related failure of NIV. A large variety of interfaces are presently available ranging from the simple nasal or oronasal mask to the helmet recently proposed [17, 18]. To our knowledge, the efficacy of these different interfaces has essentially been tested in clinical trials or in bench studies based upon the comparison of clinical indexes such as breathing pattern, airway pressure, neuromuscular drive, inspiratory muscle effort, work of breathing (WOB), arterial blood gases and dyspnea [1, 9-16]. All these interfaces allow successful non-invasive ventilation. Especially, clinical efficacy was not found different during NIV conducted with interfaces whose volumes very much differed [1, 9, 10, 16]. Only WOB and inspiratory muscle effort were slightly less decreased with the helmet, by comparison to the other interfaces [10, 16] but these differences were abolished by a specific ventilator setting [16]. In first view, this fact is surprising since some of these interfaces have a large internal volume associated with dead space that should not permit successful ventilation. In theory, the dead

space should remain as small as possible because any increase of it, induces a raise in patient's WOB [19].

We presently postulate that due to the streaming effects of the gas passing throughout the interface, the effective dead space of the interface could be quite different from the volume delimited by the interface and the part of the body embedded in this interface (called interface gas region). To test this assumption, we used numerical simulations with computational fluid dynamic (CFD) software to describe pressure, flow and gas composition in four types of interfaces regularly used to deliver NIV in the intensive care unit (ICU). In contrast with clinical trials, CFD presents the advantage to test this set of interfaces in strictly identical conditions. In a previous *in vitro* bench study, Saatci and *al*.[20] estimated the interface dead space without flow or pressure measurements. However, these authors tested several face masks but not the helmet interface.

## MATERIAL AND METHOD

We studied four interfaces commonly used in ICU (see Table 1 for interface characteristics): two oronasal face masks (masks #1 and #2), an integral mask (mask # 3) and a helmet-type interface which covers the entire head and neck (mask # 4). Each interface was successively positioned upon the same adult mannequin head made of polystyrene. Each set-up, i.e., the mannequin-interface, was numerically reconstructed in three dimensions by using computed tomography (CT) images. In each three dimensional (3D) geometry, breathing flow was simulated for successive cycles (i.e. inspiratory + expiratory phases) by using CFD software (FLUENT® Fluent Inc., Lebanon, TN, USA) until an "equilibrium state" was reached. The equilibrium state is defined as the moment where the parameters (i.e., pressure, flow and gas composition) become identical from one breathing cycle to the next breathing cycle. Details about 3D reconstruction and CFD procedure are described in the online

inserm-00595406, version 1 - 24 May 2011

electronic supplementary material (ESM). The inspiratory phase consisted of blowing a constant 600 ml/sec flow rate during 1.25 sec through the inlet of the interface. The expiratory phase consisted of blowing a constant 300 ml/sec flow rate during 2.5 sec through the mouth of the mannequin. This setting corresponds to a breathing pattern of 750 ml tidal volume ($V_T$), 16 beats/min frequency and a ratio of 2 between inspiratory and expiratory times. During the inspiratory phase, the insufflated gas called "fresh air" was normal air, fully humidified and heated at 37°C (Figure 1). During the expiratory phase, the gas blown in the interface, called in Figure 1 "exhaled air", was air enriched with $CO_2$ (see Table 2 for the exact compositions of fresh air and exhaled air). At the initial time of the first breathing cycle, the interface gas region was totally filled with fresh air. The CFD procedure allows estimating gas composition, flow and pressure at any locus of the interface gas region and at any time of the breathing cycle. Gas composition was described as the mass fraction of each gas species, especially for oxygen ($MF_{O2}$) and carbon dioxide ($MF_{CO2}$). Then, we determined the effective dead space ($V_D$) of the interface gas region defined as the rebreathed gas volume resulting from the exhaled gas trapped in this interface gas region as well as the volume of fresh air ($V_{fresh}$) that are inhaled by the mannequin during each inspiratory cycle

The pressure in the interface is composed by a mean pressure (e.g. atmospheric pressure, pressure support, positive end-expiratory pressure) and by the variation of pressure induced by the flow. This variation of pressure, which is computed by the CFD procedure, does not depend on the mean pressure as long as the thermodynamical properties of gas are not affected by the mean pressure. Therefore, our results theoretically apply to the different pressure regimes or ventilator settings, constant or intermittent, used in clinical practice during NIV.

inserm-00595406, version 1 - 24 May 2011

**RESULTS**

The equilibrium state was estimated from the time course of $MF_{O2}$ at the mouth from one cycle to the following cycle. For the first 3 interfaces shown in Table 1, the equilibrium state was quickly reached: the $MF_{O2}$ curves become identical after less than 6 breathing cycles. To reach the equilibrium state with the helmet took a little more time: approximately 2 minutes (i.e., after 32 breathing cycles).

During the inspiratory phase, $MF_{O2}$ at the mouth of the mannequin globally increases with time, while $MF_{CO2}$ decreases (see Figure 2). $MF_{O2}$ represents the quantity of oxygen available for the lung at the equilibrium state while $MF_{CO2}$ quantifies the amount of CO2 rebreathing. With the two oronasal masks (#1 and #2), that are the smaller, the $MF_{O2}$ tended to reach the maximum theoretical value (22.2%, i.e., the oxygen concentration of the total fresh air) by the end of the inspiration time. By contrast, with the two other interfaces (#3 integral and #4 helmet), $MF_{O2}$ at the mouth of the mannequin was never above 20% during the inspiratory cycle. The $MF_{CO2}$ behaviour was to decrease throughout the inspiratory phase from its maximum value (7.2%) to zero (0%) for the two oronasal masks, and to remain always positive for the two other masks: 2.4% for integral mask and 3.2% for helmet, (see Figure 2).

The effective dead space characterizing the four interfaces varied from 110 ml to 370 ml (see Figure 3). The larger $V_D$ corresponds to the helmet, and represents only 4% of the volume of the interface gas region. In this case, the effective dead space increases linearly with time and inspired volume (see Figure 4). The smallest $V_D$ was obtained with the oronasal mask #1 which has the smallest interface gas volume, and the $V_D$ was about 100% of the interface gas volume (see Figure 3). For this oronasal mask #1, $V_D$ was attained within the first 0.35 sec of the inspiratory cycle, before following a plateau during the remaining of the cycle (see Figure 4). The two others masks i.e., oronasal mask #2 and integral mask, behaved

inserm-00595406, version 1 - 24 May 2011

intermediately. The VD profile (see Figure 3) of oronasal mask # 2 during the inspiration was close to that of oronasal mask # 1, with a VD reaching 93% of the interface gas volume. The integral mask behaviour was not far from that of helmet, with a VD equal to only 35% of the interface gas volume (see Figure 3).

For all tested interfaces, the pressure field was found relatively homogeneous with a maximum pressure variation not exceeding 0.3 cm $H_2O$.

**DISCUSSION**

The main finding of this study is that the effective dead space, which is never higher than the interface gas volume, can be much smaller due to the streaming effect presently calculated by CFD. For all the interfaces the effective dead space was under 370 ml for a tidal volume of 750 ml. This is of clinical interest because it suggests that even interfaces with extremely high internal volumes (10 liters) might yet be used in patients. This holds true to the extent that patients are capable to inhale an inspired gas slightly enriched with $CO_2$ (a maximum 2.1% of $CO_2$ in volume for the helmet). The finding that effective interface dead space is not linked to the interface gas volume is consistent with several clinical studies. These studies have reported a lack of differences, in terms of patient's respiratory effort, breathing pattern and gas exchange, among interfaces with disparate internal volumes [1, 9, 14, 16, 21, 22].

Importantly, our results also show that with a tidal volume of 750 ml, the less voluminous mask (oronasal mask #1) clearly remains the most favorable in terms of re-breathing, since the VD is reduced by a factor of 3.4 when compared to the VD of the most voluminous masks (helmet) (Figure 3). Nevertheless, this beneficial effect decreases quasi linearly as tidal volume decreases (Figure 4). For example, with a tidal volume of 400 ml, the previous factor is as low as 1.8. This means that the choice of an interface based only on the

inserm-00595406, version 1 - 24 May 2011

effective $V_D$, is probably questionable. Factors such as comfort, tolerance and leaks should also be taken into account during the decision-making process.

In the extreme case of tidal volumes below 200 ml, the most efficient interface in terms of re-breathing becomes the most voluminous (the helmet). Of course, such a small tidal volume does not fit standard adult ventilation. However, if we consider the non-invasive high-frequency oscillatory ventilation at low tidal volume, as recently proposed in neonatalogy [23], our results suggest that a helmet interface could be potentially more effective than a nasal or oronasal interface due to the lower $CO_2$ rebreathing. It is not in disagreement with the fact that the helmet is not the interface of choice for NIV in COPD patients with acute exacerbation. Indeed, a 200 ml tidal volume is too low in breathing adult COPD patients to results in adequate alveolar ventilation. With these patients the required tidal volume is higher, i.e., in range where the helmet is the less efficient interface in terms of re-breathing.

The streaming effect behind effective dead space can be physically understood on the basis of the ratio between tidal volume and interface gas volume. When the interface gas volume is much larger than the tidal volume, the convective flows are reduced and the gas composition in the interface, i.e., the mass fraction of each gas species, is poorly affected by a single breathing cycle. The quasi-constancy of $MF_{O2}$ and $MF_{CO2}$ at the mouth in the helmet mask throughout the entire inspiratory phase illustrates this phenomenon (Figure 2). This assumption was already implicitly developed by Taccone *et al.* [15] who described the helmet functions as a semi-closed environment. Accordingly, the corresponding mass fraction becomes, at the equilibrium point, the mean between the mass fractions of fresh air and exhaled air and the $V_D$ is half the tidal volume, (*e.g.,* $V_D$ = 49% of $V_T$ in the helmet). On the

inserm-00595406, version 1 - 24 May 2011

basis of a negligible convective flow it suggests that this result ($V_D \cong 50\%$ of $V_T$) may be generalized to the other helmets.

By contrast, when the interface volume is small as compared to the tidal volume (oronasal mask #1 and #2), the convective flows are important. In this scenario, the recirculation velocities are relatively high and are also present in the quasi-totality of the interface gas region. In this case, the interface gas volume is washed out by the breathing flow (i.e., both the inhaled and the exhaled gas) and the dead space gets closer to the interface internal volume, (*e.g.*, 100 % of the interface gas volume for the oronasal mask # 1 and 93 % for the oronasal mask #2). On this basis, we can predict that the "small" masks (oronasal) have a $V_D$ close to their internal volume.

With the integral mask, where the gas entry is at the level of the chin, the role of convection is intermediate and the tidal volume is close to the interface gas volume. In the first part of an inspiration, (i.e., for the first 0.35 sec, corresponding to about 200 ml of inspired gas), the inferior part of the mask (from the chin to the mouth) is rapidly washed out. During this time, $MF_{O2}$ and $V_D$ are close to the values observed with the 2 smallest masks (see oronasal masks #1 and #2 in Figure 2 and 4). After this short period of time, $MF_{O2}$ at the mouth reaches a plateau resulting from gas mixture made of the gas flow coming directly from the ventilator (fresh air) and partial entrainment of the gas residing between the mouth and forehead (see the video showing the time course of the $MF_{O2}$ during the inspiration and expiration in the online ESM). The fact, that $V_D$ is impacted by both convective and diffusive phenomena, suggests that the results of our simulation cannot be generalized to the other integral mask to predict the $V_D$. Changing geometry may change the balance between convective and diffusion phenomena that will result in a different $V_D$.

Noteworthy, the physical streaming effects do not require important pressure variations in the interface gas region. It confirms that these interfaces are slightly resistive and

inserm-00595406, version 1 - 24 May 2011

are not responsible for a significant amount of resistive work. Chiumello *et al.* [10] found that helmet induced an increase of WOB associated with an increase of the time to reach the pressure support without any increase of the tidal volume while Vargas *et al.* [16] found that using a specific settings (increase of the pressure support and PEEP with the highest pressurization rate) allowed to abolish this greater inspiratory muscle effort. It suggests that this increased WOB observed with the helmet is explained in part by trigger and pressurization difficulties and not only to a large dead space problem. Such assumption is in agreement with the relative low value of $V_D$ that we obtained.

The present findings can be partially extended to clinically-relevant changes in oxygen and carbon dioxide concentrations. In this study we used normal air, heated and humidified, as inspiratory gas and we used air enriched with 5% of $CO_2$ as the expired gas. Oxygen-therapy as well as $O_2$ - $CO_2$ exchange within the lung modify gas composition. As long as physical and thermodynamic properties of the gas are not affected by gas composition and/or temperature, the effective dead space inferred in this study remains unchanged. This means that if convective and diffusive phenomena are unchanged, the effective dead space is also unchanged. Considering the slight modification in thermodynamic properties of the gas (less than 10% for gas density and less than 4% for gas kinematic viscosity) induced by either a variation of $O_2$ concentration (from 15% to 100%) or a variation of $CO_2$ concentration (from 0 to 5%), we can postulate that our results remain valid whatever the oxygen-therapy level administered. Note that, a change in $O_2$ concentration in the fresh air only requires changing the maximal and minimal values corresponding to fresh and exhaled air, in the scales of Figure 2.

One of the limitations of this study was that the numerical tool did not allow us to simulate non-intentional leak. Nevertheless, it is clear that a bias-flow leak tends to decrease

inserm-00595406, version 1 - 24 May 2011

the rebreathing problem, but it also tends to induce auto-triggering and to decrease the effective tidal volume inspired by the patient [24, 25]. However, the importance of these phenomena is extremely contingent upon a set of conditions as ventilator mode, trigger algorithms or maximum flow deliverable by the ventilator. Another limitation of this study is that we implicitly assumed the rigidity of the wall interface. This assumption is particularly questionable with the helmet. However, a recent study [16] concluded that increasing both pressure-support level and positive end-expiratory pressure may be clinically advisable when providing NIV via a helmet. Such a higher pressurization, that reduces the compliance of the helmet, tends to justify our rigidity assumption.

In summary, we have shown that mathematical modelling and computational fluid dynamics can estimate the effective dead space of NIV interfaces by analysing the pressure field/flow pattern and variations in gas composition inside these interfaces. New research efforts will be dedicated in the future to the translation of these mathematical modelling to clinical environments so as to increase efficiency while decreasing the side-effects of the clinical treatments. The effective dead space of the interfaces used for NIV was not directly related to the internal volume of the interface. For the most voluminous interfaces, effective dead space is limited to half the tidal volume while the effective dead space is close to the interface gas volume only for the less voluminous interfaces. These findings allow physicians to choose among a large number of masks which may be suitable for an individual patient and also allow physicians to take into consideration other parameters such as comfort and synchrony when choosing an interface.

inserm-00595406, version 1 - 24 May 2011

**LEGEND OF FIGURES**

Figure 1

Schematic of the set-up showing the interface positioned on the polystyrene mannequin head. CFD: Computational fluid dynamics

Figure 2

Evolution of the Mean Mass Fraction of Oxygen ($MF_{O2}$ on left vertical axis) and Carbon dioxide ($MF_{CO2}$ on right vertical axis) at the mouth of the mannequin during the inspiratory period once the equilibrium state is reached between two successive cycles (see text). The inspiration begins at time (t= 0) and stops at time (t = 1.25 sec). Dashed lines indicate the mass fractions of fresh and exhaled air.

Figure 3

Effective dead space volume, volume of inspired fresh air and interface gas volume for the four masks presented in Table 1. These data are given once the equilibrium state is reached between two successive cycles.

Figure 4

Evolution of the effective dead space volume during the inspiratory period once the equilibrium state is reached between two successive cycles. The inspiratory flow begins at time (t= 0) and stops at time (t= 1.25 sec).

inserm-00595406, version 1 - 24 May 2011

REFERENCES


1. Tarabini Fraticelli A, Lellouche F, L'Her E, Taille S, Mancebo J, Brochard L, (2009) Physiological effects of different interfaces during noninvasive ventilation for acute respiratory failure. Crit Care Med 37: 939-945
2. Mehta S, Hill NS, (2001) Noninvasive ventilation. Am J Respir Crit Care Med 163: 540-577
3. Brochard L, Mancebo J, Wysocki M, Lofaso F, Conti G, Rauss A, Simonneau G, Benito S, Gasparetto A, Lemaire F, et al., (1995) Noninvasive ventilation for acute exacerbations of chronic obstructive pulmonary disease. N Engl J Med 333: 817-822
4. Nava S, Ambrosino N, Clini E, Prato M, Orlando G, Vitacca M, Brigada P, Fracchia C, Rubini F, (1998) Noninvasive mechanical ventilation in the weaning of patients with respiratory failure due to chronic obstructive pulmonary disease. A randomized, controlled trial. Ann Intern Med 128: 721-728
5. Carlucci A, Richard JC, Wysocki M, Lepage E, Brochard L, (2001) Noninvasive versus conventional mechanical ventilation. An epidemiologic survey. Am J Respir Crit Care Med 163: 874-880
6. Girault C, Briel A, Hellot MF, Tamion F, Woinet D, Leroy J, Bonmarchand G, (2003) Noninvasive mechanical ventilation in clinical practice: a 2-year experience in a medical intensive care unit. Crit Care Med 31: 552-559
7. Robino C, Faisy C, Diehl JL, Rezgui N, Labrousse J, Guerot E, (2003) Effectiveness of non-invasive positive pressure ventilation differs between decompensated chronic restrictive and obstructive pulmonary disease patients. Intensive Care Med 29: 603-610
8. Chiumello D, (2006) Is the helmet different than the face mask in delivering noninvasive ventilation? Chest 129: 1402-1403
9. Cuvelier A, Pujol W, Pramil S, Molano LC, Viacroze C, Muir JF, (2009) Cephalic versus oronasal mask for noninvasive ventilation in acute hypercapnic respiratory failure. Intensive Care Med 35: 519-526
10. Chiumello D, Pelosi P, Carlesso E, Severgnini P, Aspesi M, Gamberoni C, Antonelli M, Conti G, Chiaranda M, Gattinoni L, (2003) Noninvasive positive pressure ventilation delivered by helmet vs. standard face mask. Intensive Care Med 29: 1671-1679
11. Mortimore IL, Whittle AT, Douglas NJ, (1998) Comparison of nose and face mask CPAP therapy for sleep apnoea. Thorax 53: 290-292
12. Navalesi P, Fanfulla F, Frigerio P, Gregoretti C, Nava S, (2000) Physiologic evaluation of noninvasive mechanical ventilation delivered with three types of masks in patients with chronic hypercapnic respiratory failure. Crit Care Med 28: 1785-1790
13. Pelosi P, Severgnini P, Aspesi M, Gamberoni C, Chiumello D, Fachinetti C, Introzzi L, Antonelli M, Chiaranda M, (2003) Non-invasive ventilation delivered by conventional interfaces and helmet in the emergency department. Eur J Emerg Med 10: 79-86
14. Racca F, Appendini L, Gregoretti C, Stra E, Patessio A, Donner CF, Ranieri VM, (2005) Effectiveness of Mask and Helmet Interfaces to Deliver Noninvasive Ventilation in a Human Model of Resistive Breathing. J Appl Physiol
15. Taccone P, Hess D, Caironi P, Bigatello LM, (2004) Continuous positive airway pressure delivered with a "helmet": effects on carbon dioxide rebreathing. Crit Care Med 32: 2090-2096
16. Vargas F, Thille A, Lyazidi A, Campo FR, Brochard L, (2009) Helmet with specific settings versus facemask for noninvasive ventilation. Crit Care Med 37: 1921-1928


inserm-00595406, version 1 - 24 May 2011

17. Antonelli M, Conti G, Pelosi P, Gregoretti C, Pennisi MA, Costa R, Severgnini P, Chiaranda M, Proietti R, (2002) New treatment of acute hypoxemic respiratory failure: noninvasive pressure support ventilation delivered by helmet--a pilot controlled trial. Crit Care Med 30: 602-608
18. Bellani G, Patroniti N, Greco M, Foti G, Pesenti A, (2008) The use of helmets to deliver non-invasive continuous positive airway pressure in hypoxemic acute respiratory failure. Minerva Anestesiol 74: 651-656
19. Lellouche F, Maggiore SM, Deye N, Taille S, Pigeot J, Harf A, Brochard L, (2002) Effect of the humidification device on the work of breathing during noninvasive ventilation. Intensive Care Med 28: 1582-1589
20. Saatci E, Miller DM, Stell IM, Lee KC, Moxham J, (2004) Dynamic dead space in face masks used with noninvasive ventilators: a lung model study. Eur Respir J 23: 129-135
21. Anton A, Tarrega J, Giner J, Guell R, Sanchis J, (2003) Acute physiologic effects of nasal and full-face masks during noninvasive positive-pressure ventilation in patients with acute exacerbations of chronic obstructive pulmonary disease. Respir Care 48: 922-925
22. Gregoretti C, Confalonieri M, Navalesi P, Squadrone V, Frigerio P, Beltrame F, Carbone G, Conti G, Gamna F, Nava S, Calderini E, Skrobik Y, Antonelli M, (2002) Evaluation of patient skin breakdown and comfort with a new face mask for non-invasive ventilation: a multi-center study. Intensive Care Med 28: 278-284
23. Colaizy TT, Younis UM, Bell EF, Klein JM, (2008) Nasal high-frequency ventilation for premature infants. Acta Paediatr 97: 1518-1522
24. Fauroux B, Leroux K, Desmarais G, Isabey D, Clement A, Lofaso F, Louis B, (2008) Performance of ventilators for noninvasive positive-pressure ventilation in children. Eur Respir J 31: 1300-1307
25. Louis B, Leroux K, Isabey D, Fauroux B, Lofaso F, (2009) Effect of manufacturers inserted mask leaks on ventilator performance. Eur Respir J 35: 627-636

inserm-00595406, version 1 - 24 May 2011

Table 1 Non invasive ventilation interfaces

| Mask | Name / Compagny | Mask type | Interface volume (ml) |
|---|---|---|---|
| # 1 | Airvie / Peters | oronasal | 111 |
| # 2 | Full Face / Koo | oronasal | 205 |
| # 3 | Inspir'aid / Fernez-Bacou | integral mask | 978 |
| # 4 | Castor-R / Starmed | helmet | 10220 |

Non invasive ventilation interfaces. The interface volume is the internal volume of each interface estimated in presence of the mannequin head.

Table 2 Gas compositions

| | | $N_2$ | $O_2$ | Ar | $CO_2$ | $H_2O$ |
|---|---|---|---|---|---|---|
| Inspiratory flow (fresh air) | Mass Fraction (%) | 72.5 | 22.2 | 1.2 | 0.0 | 3.9 |
| | Volume Fraction (%) | 73.3 | 19.7 | 0.9 | 0.0 | 6.2 |
| Expiratory flow (exhaled air) | Mass Fraction (%) | 71.1 | 16.6 | 1.2 | 7.2 | 3.9 |
| | Volume Fraction (%) | 73.3 | 15.0 | 0.9 | 4.7 | 6.2 |

inserm-00595406, version 1 - 24 May 2011

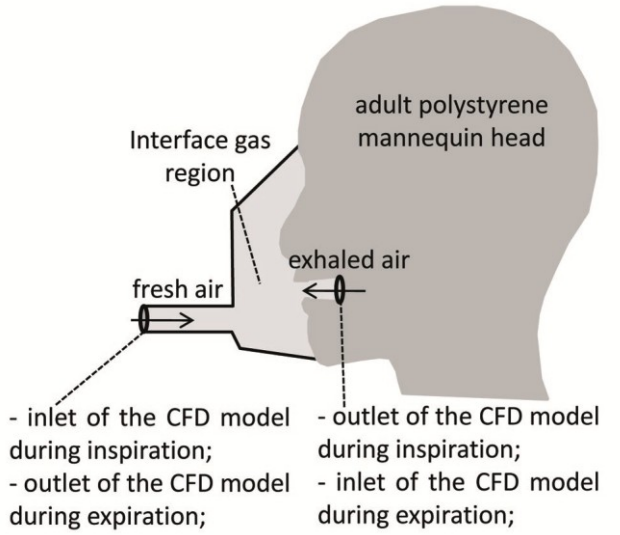


Figure1

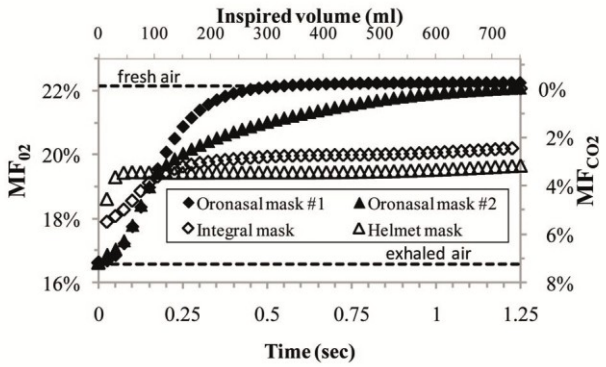


Figure2

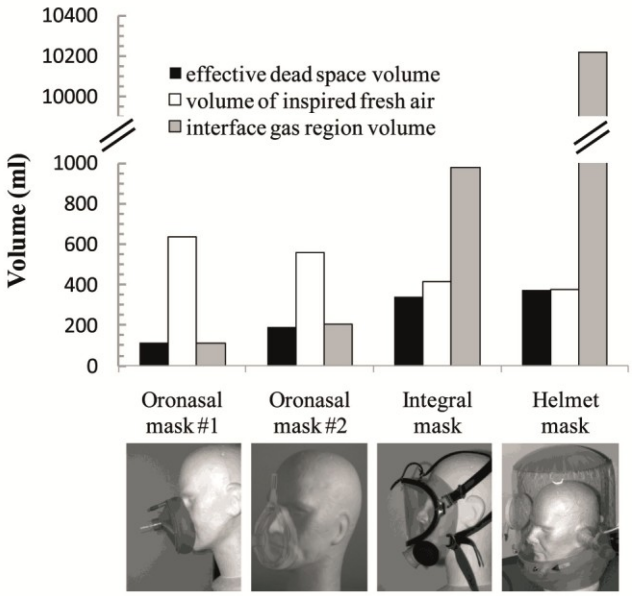


Figure 3

inserm-00595406, version 1 - 24 May 2011

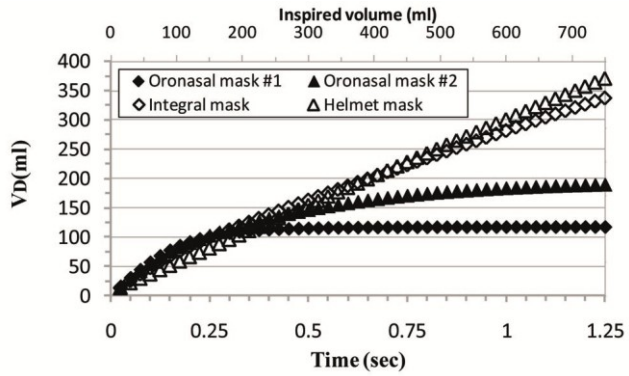


Figure 4

inserm-00595406, version 1 - 24 May 2011

# COMPARISON OF PATIENT-VENTILATOR INTERFACES BASED ON THEIR COMPUTERIZED EFFECTIVE DEAD SPACE

R. Fodil[1,2], F. Lellouche[3], J. Mancebo[4], G. Sbirlea-Apiou[1,2], D. Isabey[1,2], L. Brochard[1,2,5], B. Louis[1,2]

(1) Inserm Unite U955, Cell and Respiratory Biomechanics Group, Créteil, F-94010, France ;
(2) Université Paris-Est, Faculté de Médecine, UMR_S955, Créteil, F-94010, France ;
(3) Université Laval, Centre de Recherche de l'Institut Universitaire de Cardiologie et de Pneumologie de Québec, G1V4G5 Québec, QC, Canada ;
(4) Servei Medicina Intensiva, Hospital Sant Pau, Barcelona, Spain
(5) AP-HP, Groupe Henri-Mondor Albert-Chenevier, Service de Réanimation Médicale, Créteil, F-94010 France ;

Corresponding Author:
Bruno Louis
Inserm U955, Eq. 13
Faculté de Médecine
8 rue du général Sarrail
94010 Créteil Cedex
France

Tel: 33 1 49 81 36 76
Fax: 33 1 48 98 17 77
e-mail: bruno.louis@inserm.fr

## Online Electronic Supplementary Material

inserm-00595406, version 1 - 24 May 2011

inserm-00595406, version 1 - 24 May 2011

## THREE-DIMENSIONAL SURFACE RECONSTRUCTION AND SET-UP OF A COMPUTATIONAL FLUID DYNAMICS (CFD) PROBLEM

*Data acquisition and three-dimensional (3 D) surface reconstruction*: The 3D computational geometry used for this numerical study was derived from computed tomography (CT) scan images, except in the case of the helmet type where the interface was reconstructed using a 3D modeller (3ds Max, Autodesk, Inc., CA, USA). The same mannequin head was used to delimitate the internal volume of each interface. Scans provided contiguous axial images which were 0.5mm apart. The stack of CT images in DICOM format was imported into a commercial software package: AMIRA® (VisageImaging, Richmond, Australia) for segmentation. Segmentation assigns a label to each pixel of the image, defining whether the pixel is in a solid or in an air region of the interface. Segmentation is a prerequisite for 3D-surface model generation. We used AMIRA® software to successively construct, for each interface, a triangular surface and a volumetric tetrahedral grid of the segmented object (see Figure 1).

*Set-up of CFD problem: Mesh model.* This original mesh, Amira normal mesh (A-NM), was used in a preliminary airflow simulation. The result was used to adapt the mesh via the CFD software to resolve large pressure gradients in the flow field. The quality of the resulting mesh (F-AM) was estimated by the triangle aspect ratio (< 10) and tetra aspect ratio (< 10), as usually reported in the literature [1]. To eliminate artifacts due to the boundary conditions, we added two further elements to each model. The first was a virtual cylindrical tube of 15 cm in length and a diameter equal to the inlet interface (≈ 1.9 cm). This was situated at the junction between the interface and the ventilator circuit. The second element was a virtual elliptical duct (3.6 cm in length, a 2 cm major axis and a 1 cm minor axis) at the

outlet of the mannequin's mouth. In the case of the helmet model, a third volume, identical to the first was added at the inlet of the expiratory circuit. This was done because of the presence of two distinct circuits in the helmet interface: one for the inspiratory and the other for the expiratory flow (Figure 1, panel d).

*Set-up of CFD problem: Physical model.* The incompressible flow was chosen to be unsteady, albeit with a constant flow rate for each inspiratory/expiratory phase. Based on the value of the Reynolds number computed in the inlet circular tube (2800 in case of inspiratory flow and 1400 in case of expiratory flow), a low Reynolds number (LRN) shear stress transport (SST) $k$-ω model was used in unsteady condition. This $k$-ω model has the advantage to fit with laminar-transitional-turbulent flows. Such model has also been used for extrathoracic flow studies [2, 3]. During inspiration, a uniform velocity profile was set at the extremity of the cylindrical tube, and during expiratory flow a similar uniform velocity profile was set at the extremity of the elliptical duct. An outflow boundary condition was set at the outlet of the mesh model. During inspiration and expiration, the outlet of the mesh model was at the extremity of the elliptical duct and at the extremity of the cylindrical tube respectively. In addition, a no-slip condition was assumed at the inner walls. Inspiratory and expiratory flow cycles were simulated using constant flow rates with a temporal step of 0.025 sec.

*Set-up of CFD problem: 3D numerical model*. Inspiratory and expiratory airflows were generated in the 3D mesh model. Governing equations for momentum and mass conservation were solved by a commercial CFD software package, FLUENT® (Fluent Inc., Lebanon, TN, USA), using a control-volume based method. The solution algorithm used was a segregated solver. The governing equations were made linear with an implicit method. The local mass fraction of each gas species ($O_2$ – $CO_2$) at a given time was predicted through the solution of a

inserm-00595406, version 1 - 24 May 2011

convection-diffusion equation included in the FLUENT software. A uniform velocity profile was used as a boundary condition at the inlet of the mesh model. The CFD software package, FLUENT® (Fluent Inc., Lebanon, TN, USA), is a commercial software. It is extensively used in industry and academic fields. Our team used this software for several years. In previous studies we validated our use of this software measuring pressure drop and flow in nasal airway and human proximal airway tree [4, 5].

CFD Postprocessing: effective dead space

The CFD procedure allows estimating gas composition, flow and pressure at any locus of the interface gas region and at any time of the breathing cycle. Especially, gas composition at the mouth of the mannequin, allows determining the effective dead space ($V_D$) of the interface gas region defined as the rebreathed gas volume resulting from the exhaled gas trapped in this interface gas region. Gas composition was described from CFD estimation of the mass fraction of each gas species, especially for oxygen ($MF_{O2}$) and carbon dioxide ($MF_{CO2}$). The knowledge of the mean $MF_{O2}$ at the mouth of the mannequin (calculated via CFD as shown in the online ESM), allows to estimate the inspired volume of oxygen ($V_{O2}$):

$$V_{O2} = \int_{t_1}^{t_2} MF_{O2} \cdot \left( \frac{\rho_{air}}{\rho_{O2}} \right) \cdot \dot{V}$$

where $t_1$ and $t_2$ are the beginning and the end of the inspiratory time respectively, $\rho_{air}$ and $\rho_{O2}$ the density of air and oxygen respectively and, $\dot{V}$ is the flow rate.

$V_{O2}$ allowed to estimate the volume of fresh air ($V_{fresh}$) and the $V_D$ that are inhaled by the mannequin during each inspiratory cycle:

$$\begin{cases} V_{O2} = vF_{O2fresh} \cdot V_{fresh} + vF_{O2exhaled} \cdot V_D \\ V_T = V_{fresh} + V_D \end{cases} \Rightarrow \begin{cases} V_D = \dfrac{V_{O2} - (V_T \cdot vF_{O2fresh})}{vF_{O2exhaled} - vF_{O2fresh}} \\ V_{fresh} = V_T - V_D \end{cases}$$

inserm-00595406, version 1 - 24 May 2011

where $vF_{O2fresh}$ and $vF_{O2exhaled}$ are the volume fraction of oxygen of fresh air (heated and humidified) and exhaled air (which contains $CO_2$) respectively and, $V_T$ is the tidal volume.

References


1. Keyhani K, Scherer PW, Mozell MM, (1995) Numerical simulation of airflow in the human nasal cavity. Journal of Biomechanical Engineering 117: 429-441
2. Jayaraju S, Brouns M, Verbanck S, Lacor C, (2007) 2007, Fluid flow and particle deposition analysis in a realistic extrathoracic airway model using unstructured grids Journal of Aerosol Science 38: 494-508
3. Zhang Z, Kleinstreuer C, (2003) Low-Reynolds-number turbulent flows in locally constricted conduits: A comparison study,. AIAA journal 41: 831-840
4. Croce C, Fodil R, Durand M, Sbirlea-Apiou G, Caillibotte G, Papon JF, Blondeau JR, Coste A, Isabey D, Louis B, (2006) In Vitro Experiments and Numerical Simulations of Airflow in Realistic Nasal Airway Geometry. Ann Biomed Eng 34: 997-1007
5. de Rochefort L, Vial L, Fodil R, Maitre X, Louis B, Isabey D, Caillibotte G, Thiriet M, Bittoun J, Durand E, Sbirlea-Apiou G, (2007) In vitro validation of computational fluid dynamic simulation in human proximal airways with hyperpolarized 3He magnetic resonance phase-contrast velocimetry. J Appl Physiol 102: 2012-2023


inserm-00595406, version 1 - 24 May 2011

Figure 1

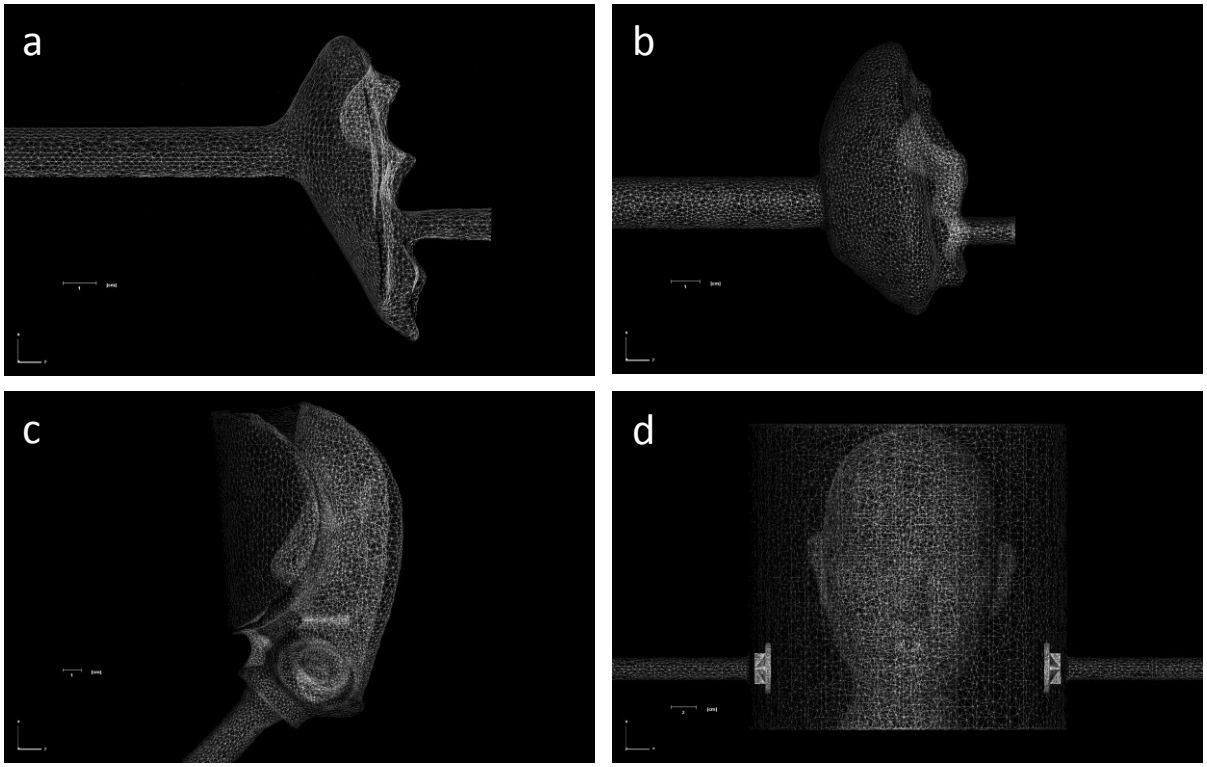


3D volumetric meshes of the 4 interfaces positioned upon the adult polystyrene mannequin head. Panel a: the oronasal mask # 1 ; Panel b: the oronasal mask #2; Panel c: the integral mask; Panel d: the helmet interface.

inserm-00595406, version 1 - 24 May 2011